THEORY OF GAIN IN GROUP-III NITRIDE LASERS

W.W. CHOW*, A.F. WRIGHT**, A. GIRNDT†, F. JAHNKE† and S.W. KOCH†
*Sandia National Laboratories, Albuquerque, NM 85718-0601, U. S. A., wwchow@sandia.gov
**Sandia National Laboratories, Albuquerque, NM 85718-0601, U. S. A.
†Department of Physics, Philipps University, Renthof 5, 35032 Marburg, Germany

ABSTRACT

A microscopic theory of gain in a group-III nitride quantum well laser is presented. The approach, which treats carrier correlations at the level of quantum kinetic theory, gives a consistent account of plasma and excitonic effects in an inhomogeneously broadened system.

INTRODUCTION

To analyze experimental results in group-III nitride lasers, it is helpful to be able to predict their gain spectra accurately. Both excitons and electron hole plasma play important roles in the optical properties of group-III nitride compounds, even under lasing conditions of high carrier density and temperature.[1] Also, inhomogeneous broadening is present, due to localization effects from dimensional or composition variations.[2] This paper describes a consistent treatment of the above factors.

THEORY

Our approach is based on a Hamiltonian that contains the Coulomb interaction energy among carriers.[3] Using this Hamiltonian and following a derivation similar to that resulting in the Semiconductor Bloch Equations, we get the equation of motion for the microscopic polarization, $p_{\vec{k}}$, due to an electron hole pair,[4, 5]

$$\frac{d}{dt}p_{\vec{k}} = -i\omega_{\vec{k}}p_{\vec{k}} - i\Omega_{\vec{k}}\left(n_{e,\vec{k}} + n_{h,\vec{k}} - 1\right) - \Gamma_{\vec{k}}p_{\vec{k}} + \sum_{\vec{q}}\Gamma_{\vec{k},\vec{q}}p_{\vec{k}+\vec{q}} \quad . \tag{1}$$

The first two terms on the right hand side describe the oscillation of the polarization at the transition frequency, $\omega_{\vec{k}}$, and the stimulated emission and absorption processes. The many-body Coulomb effects appear in the form of a carrier density, N, dependence in the transition energy,

$$\hbar\omega_{\vec{k}}(N) = \varepsilon_{e,\vec{k}} + \varepsilon_{h,\vec{k}} + [\varepsilon_{g,0} + \Delta\varepsilon_{SX}(N)] \quad , \tag{2}$$

where $\Delta\varepsilon_{SX}$ is the exchange contribution to the renormalized band gap energy. They also lead to a renormalized Rabi frequency,

$$\Omega_{\vec{k}} = \frac{1}{\hbar}\left(\mu_{\vec{k}}E + \sum_{\vec{q}}V_q p_{\vec{k}+\vec{q}}\right) \quad , \tag{3}$$

DISCLAIMER

where $\mu_{\vec{k}}$ is the optical dipole matrix element, E is the laser electric field, and V_q is the Fourier transform of the bare (unscreened) Coulomb potential. Carrier-carrier collisions give rise to the last two terms. The third term on the RHS describes diagonal polarization dephasing, with a dephasing rate,

$$\begin{aligned}\Gamma_{\vec{k}} &= \sum_{a=e,h}\sum_{b=e,h}\sum_{\vec{q}}\sum_{\vec{k}'}\frac{2\pi}{\hbar}V_q^2 D(\varepsilon_{a,\vec{k}}+\varepsilon_{b,\vec{k}'}-\varepsilon_{a,\vec{k}+\vec{q}}-\varepsilon_{b,\vec{k}'-\vec{q}}) \\ &\times\left[n_{a,\vec{k}+\vec{q}}\left(1-n_{b,\vec{k}'}\right)n_{b,\vec{k}'-\vec{q}}+\left(1-n_{a,\vec{k}+\vec{q}}\right)n_{b,\vec{k}'}\left(1-n_{b,\vec{k}'-\vec{q}}\right)\right] \quad , \end{aligned} \tag{4}$$

where $D(\Delta)=\delta(\Delta)+i\pi^{-1}P(\Delta^{-1})$, and P denotes the principle value. The last term shows a nondiagonal scattering contribution that couples polarizations with different $\vec{k}$'s. The coefficient,

$$\begin{aligned}\Gamma_{\vec{k},\vec{q}} &= \sum_{a=e,h}\sum_{b=e,h}\sum_{\vec{k}'}\frac{2\pi}{\hbar}V_q^2 D(\varepsilon_{a,\vec{k}}+\varepsilon_{b,\vec{k}'}-\varepsilon_{a,\vec{k}+\vec{q}}-\varepsilon_{b,\vec{k}'-\vec{q}}) \\ &\times\left[\left(1-n_{a,\vec{k}}\right)\left(1-n_{b,\vec{k}'}\right)n_{b,\vec{k}'-\vec{q}}+n_{a,\vec{k}}n_{b,\vec{k}'}\left(1-n_{b,\vec{k}'-\vec{q}}\right)\right] \quad . \end{aligned} \tag{5}$$

In this paper, we limit the discussion to the small signal gain, where the carrier populations, $n_{e,\vec{k}}$ and $n_{h,\vec{k}}$ are inputs to the calculations.

The polarization equations are solved numerically for the steady state solution. Using a semiclassical laser theory, the intensity gain G is given by[3] (MKS units):

$$G=-\frac{2\omega}{\varepsilon_0 n c V\mathcal{E}}\,\mathrm{Im}\left(\sum_{\vec{k}}\mu_{\vec{k}}^{*}p_{\vec{k}}e^{i\omega t}\right) \quad , \tag{6}$$

where $\mathcal{E}$ is the slowly varying electric field amplitude, ω is the laser frequency, ε_0 and c are the permittivity and speed of light in vaccuum, n is the background refractive index, V is the active region volume, and the summation is over all electron and hole states.

Equation (6) gives the homogeneously broadened gain spectrum for an ideal structure, where the quantum well thickness and composition are precisely known. On the other hand, experimental data suggest that the gain region may consist of localized regions of different quantum well thicknesses or compositions. Assuming that these regions are sufficiently large so that the quantum confinement remains only along the epitaxial direction, we can treat the effects of inhomogeneous broadening by a statistical average of the homogeneous gain spectra, i.e.,

$$G_{inh}(\omega,N,T)=\int dx\; P(x)\; G(x,\omega,N,T) \quad , \tag{7}$$

where $P(x)$ is a normal distribution representing the variation in x, which can either be the quantum well thickness or indium concentration.

RESULTS

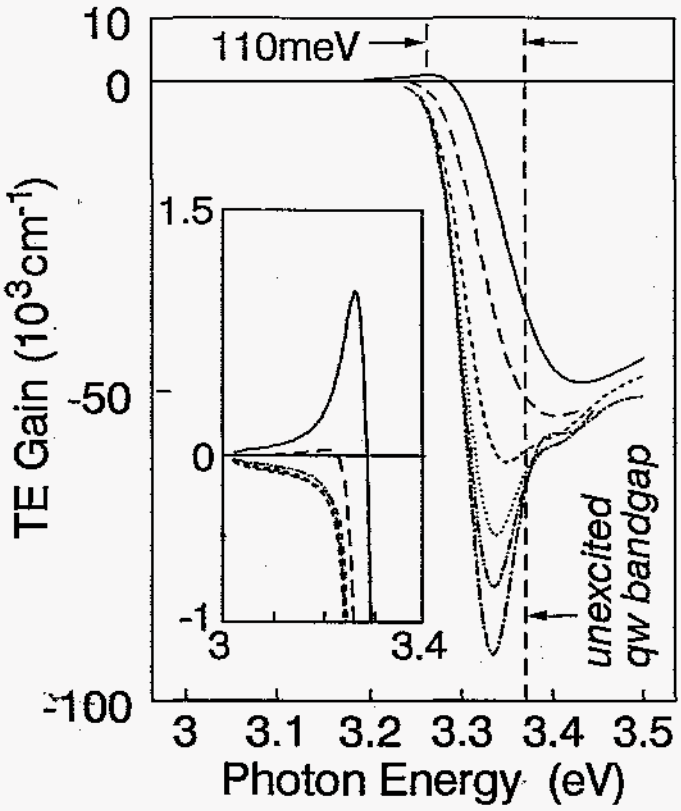

Fig. 1. Calculated TE gain spectra for a 4nm $In_{0.1}Ga_{0.9}N/Al_{0.2}Ga_{0.8}N$ quantum well at $T = 300K$ and densities N = 0.1, 0.5, 1.0, 2.0, 4.0, and 6.0×10^{12}cm^{-2}. The inset shows the gain portion of the spectra.

Figure 1 shows the computed spectra for a 4nm $In_{0.1}Ga_{0.9}N/Al_{0.2}Ga_{0.8}N$ quantum well structure and different carrier densities. The laser field polarization is in the plane of the quantum well (transverse electric or TE polarization). For the wurtzite structure considered, the orthogonal (TM) polarization has negligible gain, even at high carrier density. We use a 6×6 Luttinger-Kohn Hamiltonian and the envelope approximation[6] to compute the hole energy dispersions and optical dipole matrix elements. Input parameters are the bulk wurtzite material parameters (Table I). The ratio of the band offset (conduction/valence bands) is assumed to be 67/33. Alloy properties are obtained as composition-weighted averages of the bulk values, except for the optical bowing parameters, where we use $b = 0.53eV$ for AlGaN and $b = 1.02eV$ for InGaN.[7] The spectra are calculated assuming an inhomogeneous broadening due to a 0.01 (10%) standard deviation in the indium concentration.

Table 1. Material parameters for AlN, GaN and InN. Unless otherwise noted, the values are from density functional calculations (see Ref.[10] for details). Calculations for the crystal-field splittings and deformation potentials use the Sterne-Inkson formulation.[11].

	AlN	GaN	InN
a(Å)[10]	3.084	3.162	3.501
c(Å)[10]	4.948	5.142	5.669
C_{13}(GPa)	108	103	92
C_{33}(GPa)	373	405	224
(a_{cz}-D_1)(eV)	-4.21	-6.11	-4.05
(a_{ct}-D_2)(eV)	-12.04	-9.62	-6.67
D_3(eV)	9.06	5.76	4.92
D_4(eV)	-4.05	-3.04	-1.79
Δ_1(eV)	-.221	0.019	0.025
E_g(eV)	6.28[12]	3.50[13]	1.89[14]
Δ_0(eV)[15]	0.019	0.013	0.001
m_c^*	0.31	0.18	0.011[16]
$m_{hh}^{\parallel}$	3.52	2.01	1.89
$m_{lh}^{\parallel}$	3.52	2.01	1.89
$m_{split}^{\parallel}$	0.25	0.15	0.024
$m_{hh}^{\perp}$	21.8	2.13	2.00
$m_{lh}^{\perp}$	0.32	0.19	0.033
$m_{split}^{\perp}$	4.38	1.45	1.60

The low density spectra show an exciton resonance. The existence of excitons at the high temperature of $T = 300K$ and carrier densities up to $N = 10^{12}cm^{-2}$ is evidence of strong Coulomb attraction between electrons and holes. It is important to note that the presence of excitonic effects in our results is not due to an *ad hoc* inclusion of excitonic transitions into a free-carrier theory, as is the case for some phenomenological models.[8] Rather the presence of excitons comes about because of the attractive Coulomb potential in the Hamiltonian we use to describe the electron-hole system. The present approach gives a consistent treatment of relaxation and screening effects in a exciton/plasma system, which is not possible with phenomenological approaches that treat the excitons and plasma as non interacting.

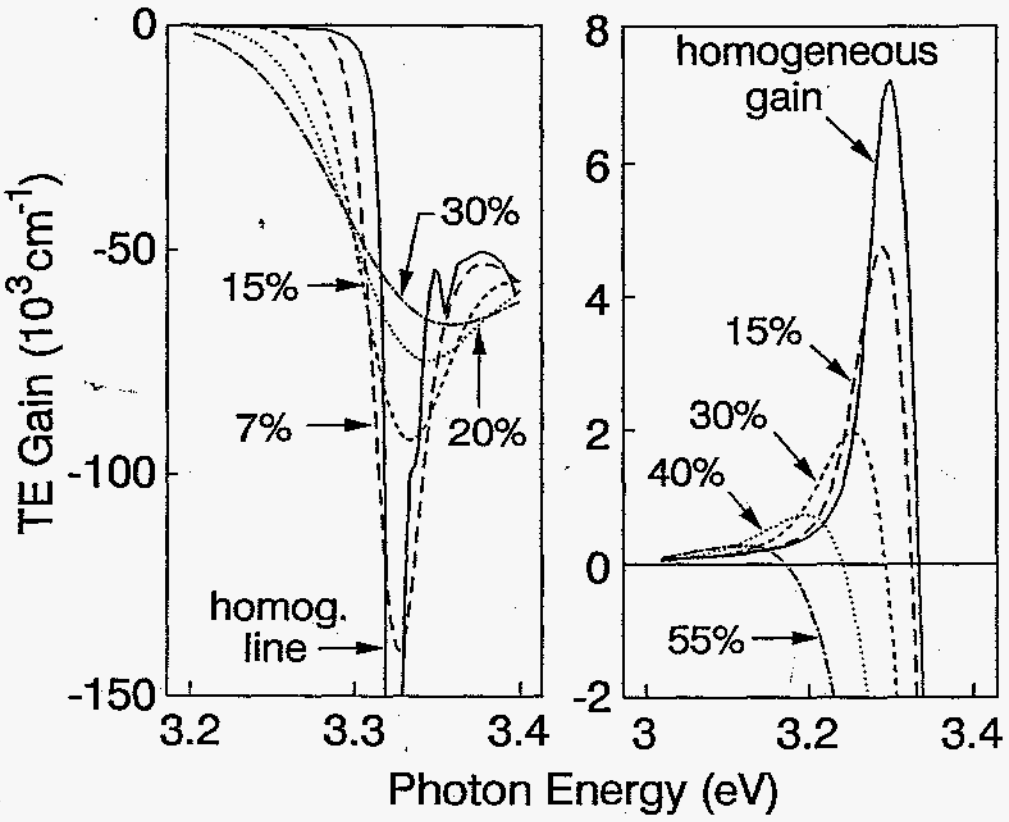

Fig. 2. TE gain/absorption spectra at N = 10^{11}cm^{-2} (left) and 8×10^{12}cm^{-2} (right). The solid curves depict the homogeneously broadened spectrum, while the other spectra are computed for increasing inhomogeneous broadening due to composition variation. All other parameters are similar to those in Fig. 1.

At high densities the exciton resonance vanishes and gain appears (see inset). Recently, there is much interest in the energy of the optical emission.[2] Our calculation shows that for the carrier density $N = 6 \times 10^{12} cm^{-2}$, which gives a local gain of $\sim 10^3 cm^{-2}$, the emission peak is over 100meV in energy lower than the unexcited quantum well bandgap energy. This red shift is the net result of the energy shifts due to several physical mechanisms. There is band filling, which leads to a blue shift that depends on the bandstructure. In addition, Coulomb interactions resulting in bandgap renormalization, Coulomb enhancement, dephasing and screening lead to a red shift, as well as reshaping of the spectrum. Finally, inhomogeneous broadening can also contribute to a significant red shift of the gain peak.

Figure 2 illustrates the effects of inhomogeneous broadening. At low densities, inhomogeneous broadening leads to broadening of the exciton resonance (Fig. 2, left). At high densities it reduces the gain, and shifts the spectrum towards lower energy (Fig. 2, right). Our calculations predict a red shift of the gain peak relative to the unexcited quantum well band gap that ranges from 70meV for the homogeneously case, to >200meV for composition variations >50% (i.e. mean indium concentration of 0.1 with standard deviation of 0.05).

Spontaneous emission spectra are more readily obtained in experiments than gain spectra. Figure 3 (top) shows the spontaneous emission spectra at carrier density $N = 5 \times 10^{12} cm^{-2}$ and different inhomogeneous broadening. The spontaneous emission spectra are obtained from the calculated gain spectra by using a relationship that is based on energy conservation arguements.[9] Comparison with the gain spectra (Fig. 3, bottom) shows that a significant energy difference can occur between spontaneous emission and gain peaks. For the homogeneously broadened spectra, the gain peak is red shifted by 40meV from the spontaneous emission. For a standard deviation of 0.03 (30%) in the indium concentration, this shift increases to >100meV, making propagation effects important in the determination of the energy of the optical emission.

CONCLUSION

In summary, we describe a theory of gain for group-III nitride quantum well lasers. The effects of excitons are integrated with those of an interacting electron-hole plasma by using a Hamiltonian for the electron-hole system that includes the many-body Coulomb interactions. The description of carrier correlation effects at the level of quantum kinetic theory gives a consistent treatment of broadening and screening effects, due to both the electron-hole plasma and the excitons. Finally, by taking into account the inhomogeneously broadening due to spatial variations in quantum well thickness or composition, we provide a realistic description of actual experimental configurations.

ACKNOWLEDGMENTS

This work was supported in parts by the U. S. Department of Energy under contract No. DE-AC04-94AL85000, the Deutsche Forschungsgemeinschaft (Germany), and the Leibniz Prize.

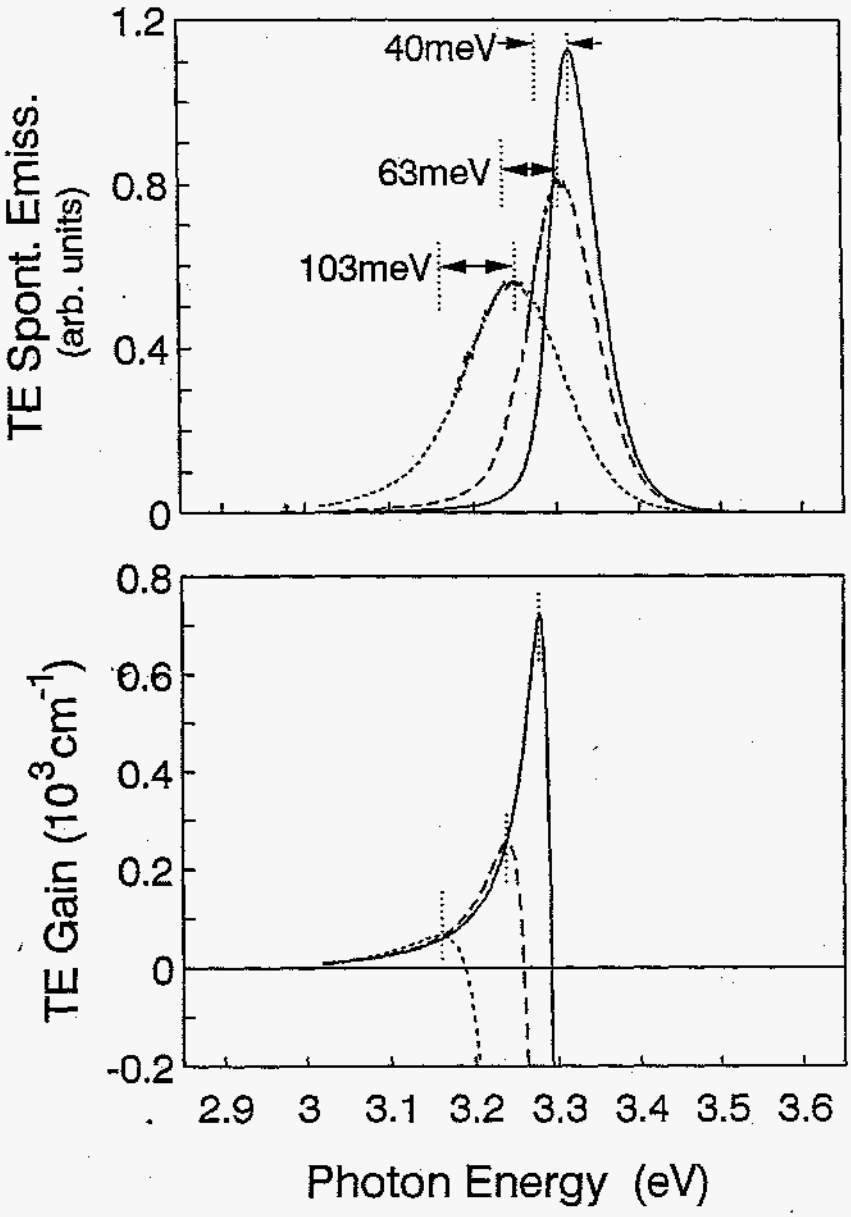

Fig. 3 Spontaneous emission (top) and gain spectra (bottom) at $N = 5\times10^{12}\text{cm}^{-2}$. The solid curves are the homogeneously broadened spectra, the long and short dashed curves have 15% and 30% variations in Indium concentrations, respectively. The energy values of 40, 63 and 103meV correspond to the energy differences between the gain and spontaneous emission peaks. All other parameters are similar to those in Fig. 1.

References

[1] W. W. Chow, A. Knorr and S. W. Koch, Appl. Phys. Letts. **67**, 754 (1995).

[2] S. Nakamura, SPIE Conference on Physics and Simulation of Opto-Electronic Devices, 8-14 Feb. 1997, San Jose, CA.

[3] W. W. Chow, S. W. Koch and M. Sargent III, Semiconductor-Laser Physics, (Springer Verlag, Berlin, 1994), p. 124.

[4] M. Lindberg and S. W. Koch, Phys. Rev. **B38**, 3342 (1988).

[5] F. Jahnke, et al, Phys. Rev. Lett. **77**, 5257 (1996).

[6] S. L. Chuang and C. S. Chang, Phys. Rev. B54 (1996).

[7] A. F. Wright and J. S. Nelson, Appl. Phys. Letts. **66**, 3051 (1995).

[8] F. Jain and W. Huang, IEEE J. Quantum Electron. 32, 859 (1996).

[9] C. H. Henry, R. A. Logan and F. R. Merritt, J. Appl. Phys. **51**, 3042 (1980).

[10] A. F. Wright and J. S. Nelson, Phys. Rev. **B51**, 7866 (1995).

[11] S. J. Jenkins, G. P. Srivastava and J. C. Inkson, Phys. Rev. **B48**, 4388 (1993).

[12] P. B. Perry and R. F. Rutz, Appl. Phys. Letts. **33**, 319 (1978).

[13] B. Monemar, Phys. Rev. **B10**, 676 (1974).

[14] T. L. Tansley and C. P. Foley, J. Appl. Phys. **59**, 3241 (1986).

[15] S. H. Wei and A. Zunger, Appl. Phys. Letts. **69**, 2719 (1996).

[16] V. A. Tyagai, A. M. Evstigneev, A. N. Krasiko, A. F. Andreeva and V. Y. Malakhov, Soviet Phys. Semicond. **11**, 1257 (1977).